Scalable Optimization Methods for Distribution Networks with High PV Integration

Swaroop S. Guggilam, Emiliano Dall'Anese, *Member, IEEE*, Yu Christine Chen, *Member, IEEE*, Sairaj V. Dhople, *Member, IEEE*, and Georgios B. Giannakis, *Fellow, IEEE*

***Abstract*—This paper proposes a suite of algorithms to determine the active- and reactive-power setpoints for photovoltaic (PV) inverters in distribution networks. The objective is to optimize the operation of the distribution feeder according to a variety of performance objectives and ensure voltage regulation. In general, these algorithms take a form of the widely studied AC optimal power flow (OPF) problem. For the envisioned application domain, nonlinear power-flow constraints render pertinent OPF problems nonconvex, and computationally-intensive for large systems. To address these concerns, we formulate a quadratic constrained quadratic program (QCQP) by leveraging a linear approximation of the algebraic power-flow equations. Furthermore, simplification from QCQP to a linearly constrained quadratic program (LCQP) is provided under certain conditions. The merits of the proposed approach are demonstrated with simulation results that utilize realistic PV-generation and load-profile data for an illustrative distribution system.**

***Index Terms*—Distribution networks, PV systems, Optimization, Linearization.**

I. Introduction

THE methods proposed in this paper seek contributions in the domain of next-generation distribution-system operations and control by leveraging scalable convex optimization approaches. The increased penetration of PV systems has highlighted pressing needs to address power quality and reliability concerns. Therefore, systematic means to operate distribution networks with high PV penetration will be key to ensure a sustainable capacity growth with limited need for transmission expansion.

Recent efforts in the domain of PV integration are focused on inverters deviating away from nominal maximum power outputs to provide reactive power support and curtail active power as required. For instance, local active power control strategies proposed in [1], [2] are grounded on the premise of curtailing active power from inverters based on the observed nodal voltages. Similarly, low power factors and possibly high network currents—which may lead to conductor overheating and power losses—can occur if local reactive-power control strategies are used [3]–[5]. Focusing on network-wide optimality, an OPF-based Optimal Inverter Dispatch (OID) strategy was proposed in [6], where the SDP relaxation for AC power flow equations (see, e.g., [7]) was leveraged to obtain a strategy to dispatch network-wide-optimal setpoints for PV inverters. However, for a balanced network with N nodes, this problem requires $\mathcal{O}(N^2)$ optimization variables; consequently, this approach may become computationally expensive as the distribution-system size grows [8], even when parallel decomposition arguments for SDP programs are advocated [9]. A notable exception is the recently proposed sparsity-exploiting SDP formulation in [10] in which number of variables do not scale as $\mathcal{O}(N^2)$. Another pertinent reference is a Second Order Cone (SOC) relaxation of the OPF problem proposed in [11]. Using the SOC relaxation, a rendition of the OPF problem for networks with approximately 3000 buses has been solved in around 30 seconds [12]. We adopt an alternate perspective to tackle scalability in this work. In contrast to the relaxations advocated in the references above, we focus on obtaining linear relationships between network voltages and nodal power injections, which bypasses non-convexity in OPF problems and yields a convex problem formulation. In particular, we propose a Scalable Optimal Inverter Dispatch algorithm (SOID) using a recently proposed linear approximation to the power flow equations [13], [14]. This problem formulation address a different suite of Optimal Power Flow problems, wherein along with voltage we also find active- and reactive-power setpoints for PV inverters. The proposed schemes required only $\mathcal{O}(N)$ optimization variables, and leads to a convex Linearly Constrained Quadratic Program (LCQP). Furthermore, when the cost is linear and real-power (or reactive-power) compensation alone is implemented, the SOID is in fact a linear program.

A key insight that this paper leverages to develop the optimization problems is a linear approximation of the nonlinear power flow expressions in rectangular coordinates [13], [14]. A variety of methods exploiting linearizations of the nonlinear power flow equations have been proposed in the literature. For instance, linear non iterative power flow algorithms considering only active power flows are proposed in [15], [16]. Relaxed AC OPF problems obtained by linearizing just the power flow balance equations have been proposed in [17]–[20]. Different from the approaches above, we leverage a closed-form linear approximation for the voltages across the network [13], [14] to formulate computationally tractable optimization problems.

S. S. Guggilam, S. V. Dhople and G. B. Giannakis were supported in part by the National Science Foundation through grants CCF 1423316, CyberSEES 1442686, and CAREER award ECCS-1453921; and by the Institute of Renewable Energy and the Environment, University of Minnesota under grant RL-0010-13; The work of E. Dall'Anese was supported in part by the Laboratory Directed Research and Development Program at the National Renewable Energy Laboratory.

S. S. Guggilam, S. V. Dhople and G. B. Giannakis are with the Department of Electrical and Computer Engineering, and the Digital Technology Center, University of Minnesota, Minneapolis, MN 55455, USA. E-mail: {guggi022, sdhople, georgios}@umn.edu. E. Dall'Anese is with the National Renewable Energy Laboratory, Golden, CO. E-mail: emiliano.dallanese@nrel.gov. Y. C. Chen is with the Department of Electrical and Computer Engineering, University of British Columbia, Vancouver, British Columbia V6T 1Z4. E-mail: chen@ece.ubc.ca

Compared to semidefinite programming (SDP) methods in our original work [6], simulations for the IEEE 123-node system for an equivalent QCQP demonstrate substantial computational speed improvements, which will be discussed in the case studies. Furthermore, we remark that while we consider single-phase settings, the linear approximations for the solutions to the power flow problem can be extended to cover multi-phase setups, following which, adopting approaches akin to the ones in [15], [17], [21], the methods proposed here can be tailored to multi-phase setups. While these optimization problems for multi-phase settings are beyond the scope of this manuscript, they present compelling options for future work.

To further promote customer privacy while guaranteeing scalability of the algorithms with limited information exchanges, we also propose a distributed version of the problem setup leveraging the alternating direction method of multipliers (ADMM) [22]–[24]. Convergence is faster if ADMM is implemented in comparison to other distributed solution approaches such as the sub-gradient method [25], [26]. The SOID problem discussed above can be decomposed as a sum of utility optimization and customer based optimization objectives. Utility optimization includes network performance objectives like power losses, whereas customer based optimization includes maximizing their monetary objectives (e.g., minimizing the amount of active power to be curtailed). A two-way exchange of information is required to implement the above setup. Once the optimal setpoints are computed, they are dispatched to inverters, where we assume that local regulation capability implements the desired output real and reactive power.

To summarize, the contributions of this paper are as follows. First, we leverage a linearized version of the power flow equations in rectangular coordinates tailored to distribution networks to formulate an OPF-type problem with direct applications to distribution networks with PV systems. The formulated SOID problem (and accompanying special case tailored for resistive-dominant networks) can be formulated to meet performance objectives of minimizing power losses and voltage deviations from the nominal. Finally, to further improve computational performance and promote scalability, we propose a distributed version of the problem that can be solved with ADMM.

The remainder of this paper is organized as follows. In Section II, set of notations and network model used throughout the paper are described, and an approximate expression for the voltages is derived from linearization of the power-flow equations expressed in rectangular coordinates. Section III presents the SOID problem formulation along with the distributed implementation leveraging ADMM. In Section IV, we provide various case studies and simulation results to demonstrate the applicability of the method, and demonstrate computational savings compared to our previous efforts that leveraged SDP relaxations of the OPF problem. Finally concluding remarks and pertinent directions for future work are highlighted in Section V.

II. Preliminaries and Power System Model

In this section, we first establish notation and then describe the power-system model that is utilized in the remainder of the manuscript. We also develop the linearized model for the voltages in the network.

A. Notation

The matrix inverse is denoted by $(\cdot)^{-1}$, transpose by $(\cdot)^{\mathrm{T}}$, complex conjugate by $(\cdot)^{*}$, real and imaginary parts of a complex number by $\mathrm{Re}\{\cdot\}$ and $\mathrm{Im}\{\cdot\}$, respectively, magnitude and phase of a complex scalar by $|\cdot|$ and $\angle(\cdot)$, respectively and $\mathrm{j} := \sqrt{-1}$. A diagonal matrix formed with entries of vector x is denoted by $\mathrm{diag}(x)$. A diagonal matrix formed with the lth entry given by x_l/y_l is denoted by $\mathrm{diag}(x/y)$, where x_l and y_l are the lth entries of the vectors x and y, respectively and a diagonal matrix with the lth entry given by x_l^{-1} is denoted as $\mathrm{diag}(1/x)$. For a matrix X, X_{mn} returns the entry in the m row and n column of X. The $N \times 1$ vectors with all ones and all zeros are denoted by 1_N and 0_N. The spaces of $N \times 1$ real-valued and complex-valued vectors are denoted by $\mathbb{R}^N$ and $\mathbb{C}^N$, respectively; $\mathbb{T}^N$ denotes the N-dimensional torus.

B. Network Model

Consider a single-phase distribution network with $N+1$ nodes collected in the set $\mathcal{N}$ and distribution lines collected in the set $\mathcal{E}$. Set $\mathcal{N}' \subset \mathcal{N}$ excludes the $N+1$th node, i.e., $\mathcal{N}' = \mathcal{N} \setminus \{N+1\}$. At H of these $N+1$ nodes (collected in the set $\mathcal{H}$), we assume PV systems are installed with inverters capable of responding to real- and reactive-power dispatch commands. The $N+1$ node models the secondary of the step-down distribution transformer, and is assumed to be the slack bus. Lines are represented by the set of edges $\mathcal{E} := \{(m,n)\} \subset \mathcal{N} \times \mathcal{N}$. Finally, note that $(\cdot)_{(m,n)}$ represents a signal corresponding to the (m,n) line.

Let $I = [I_1, \ldots, I_N]^{\mathrm{T}}$, $V = [V_1, \ldots, V_N]^{\mathrm{T}} \in \mathbb{C}^N$ and $S = [S_1, \ldots, S_N]^{\mathrm{T}}$ where $I_\ell \in \mathbb{C}$ denotes the current injected into bus ℓ, $V_\ell = |V|_\ell \angle \theta_\ell \in \mathbb{C}$ represents the voltage phasor at bus ℓ and $S_\ell = P_\ell + \mathrm{j}Q_\ell$ denotes the complex-power bus injected at bus ℓ. In rectangular coordinates, we have $V = V_{\mathrm{re}} + \mathrm{j}V_{\mathrm{im}}$, where $V_{\mathrm{re}}, V_{\mathrm{im}} \in \mathbb{R}^N$ denote the real and imaginary components of V. Further we will define $|V| = [|V|_1, \ldots, |V|_N]^{\mathrm{T}} \in \mathbb{R}^N_{>0}$ and $\theta = [\theta_1, \ldots, \theta_N]^{\mathrm{T}} \in \mathbb{T}^N$, which we will use subsequently. The available active power (based on the incident irradiance) is denoted by the vector $P_{\mathrm{av}} \in \mathbb{R}^N_{\geq 0}$. The active power curtailed by the inverters are collected in P_{c}; and Q_{c} collects the reactive powers generated/consumed by the PV inverters. Active- and reactive- power loads are collected in P_{d} and Q_{d} respectively.

The electrical network operation in sinusoidal steady state is described by Kirchhoff's current law as follows:

$$\begin{bmatrix} I \\ I_{N+1} \end{bmatrix} = \begin{bmatrix} Y & \overline{Y} \\ \overline{Y}^{\mathrm{T}} & \tilde{y} \end{bmatrix} \begin{bmatrix} V \\ V_\circ \mathrm{e}^{\mathrm{j}\theta_\circ} \end{bmatrix} \tag{1}$$

where $V_\circ \mathrm{e}^{\mathrm{j}\theta_\circ}$ is the slack-bus voltage with $V_\circ$ denoting the voltage magnitude at the secondary of the step-down transformer feeding the network. Hereafter, we will consider

$V_\circ = 1$ and $\theta_\circ = 0$ for our discussion. Dimensions of the entries of the admittance matrix are as follows: $\overline{Y} \in \mathbb{C}^N$, $Y \in \mathbb{C}^{N\times N}$, and $\tilde{y} \in \mathbb{C} \setminus \{0\}$. Also $Y = G + \mathrm{j}B$, where G and $B \in \mathbb{R}^{N\times N}$ are conductance and susceptance matrices respectively. Current injected into slack bus is given by I_{N+1}. The vector of shunt admittances can be extracted as

$$Y1_N + \overline{Y} = Y_{\rm sh} = G_{\rm sh} + \mathrm{j}B_{\rm sh} \tag{2}$$

where $Y_{\rm sh} \in \mathbb{C}^N$, $G_{\rm sh}$ and $B_{\rm sh} \in \mathbb{R}^N$. Finally, minimum and maximum voltage magnitude limits at the nodes are denoted by $V^{\min}$ and $V^{\max}$, respectively.

C. Approximate Expression for the Voltages

We begin with complex-power balance, which can be written with the aid of (1) as follows:

$$S = \mathrm{diag}\,(V)\, I^* = \mathrm{diag}\,(V)\left(Y^*V^* + \overline{Y}^*\right). \tag{3}$$

Recall that we denote: $P_{\rm av} \in \mathbb{R}^N$ as the available power (based on the incident irradiance), $P_{\rm c} \in \mathbb{R}^N$ as the active power curtailed, $P_{\rm d} \in \mathbb{R}^N$ is total load and similar definitions for reactive-power related variables. Note that entries of $P_{\rm av}$ and $P_{\rm c}$ are non-zero only if the corresponding node is connected to a PV system With these definitions in mind, it follows that:

$$S = (P_{\rm av} - P_{\rm c} - P_{\rm d}) + \mathrm{j}(Q_{\rm c} - Q_{\rm d}). \tag{4}$$

Let the actual solution to (3) be denoted by $V \in \mathbb{C}^N$. We linearize (3) by expressing $V = V_{\rm nom} + \Delta V$, where $V_{\rm nom} = |V_{\rm nom}|\angle\theta_{\rm nom} \in \mathbb{C}^N$ is some pre-defined nominal voltage vector, and ΔV captures perturbations around $V_{\rm nom}$. Consider the following choice of nominal voltage, which also corresponds to the voltage across the network with zero current injections:

$$V_{\rm nom} = -Y^{-1}\overline{Y}. \tag{5}$$

With this choice of nominal voltage, it is easy to show that by neglecting higher-order terms in (3), we get the following solution for ΔV (details are in [14]):

$$\Delta V = Y^{-1}\mathrm{diag}\,(1/V^*_{\rm nom})\, S^*. \tag{6}$$

Then, expanding the terms in (6) and considering the real and imaginary components of ΔV provides the following equations:

$$\Delta V_{\rm re} = \left(R\ \mathrm{diag}\left(\frac{\cos\theta_{\rm nom}}{|V_{\rm nom}|}\right) - X\ \mathrm{diag}\left(\frac{\sin\theta_{\rm nom}}{|V_{\rm nom}|}\right)\right)P + \left(X\ \mathrm{diag}\left(\frac{\cos\theta_{\rm nom}}{|V_{\rm nom}|}\right) + R\ \mathrm{diag}\left(\frac{\sin\theta_{\rm nom}}{|V_{\rm nom}|}\right)\right)Q, \tag{7}$$

$$\Delta V_{\rm im} = \left(X\ \mathrm{diag}\left(\frac{\cos\theta_{\rm nom}}{|V_{\rm nom}|}\right) + R\ \mathrm{diag}\left(\frac{\sin\theta_{\rm nom}}{|V_{\rm nom}|}\right)\right)P - \left(R\ \mathrm{diag}\left(\frac{\cos\theta_{\rm nom}}{|V_{\rm nom}|}\right) - X\ \mathrm{diag}\left(\frac{\sin\theta_{\rm nom}}{|V_{\rm nom}|}\right)\right)Q, \tag{8}$$

where $P = P_{\rm av} - P_{\rm c} - P_{\rm d}$ and $Q = Q_{\rm c} - Q_{\rm d}$ and $Y^{-1} = R + \mathrm{j}X$.

Notice that $|V| = |V_{\rm nom}| + \Delta V_{\rm re}$ and $\theta = \theta_{\rm nom} + \Delta V_{\rm im}$ serve as first-order approximations to the voltage magnitudes and phases across the distribution network, respectively, when $\theta_{\rm nom} \approx 0_N$. In the present setting, this is true when shunt impedances are negligible, i.e., $Y_{\rm sh} = 0_N$. Furthermore, from (2) and (5), we see that $Y1_N + \overline{Y} = 0_N$, and $|V_{\rm nom}| = 1_N$; as a result of which (7) and (8) simplify as below:

$$\Delta V_{\rm re} = R\ P + X\ Q, \quad \Delta V_{\rm im} = X\ P - R\ Q. \tag{9}$$

Finally, with the above discussions and approximations in place, we recognize that the voltage magnitude at the n-th bus is approximately given by

$$|V|_n \approx 1 + \sum_{\ell\in\mathcal{N}'} R_{n\ell}P_\ell + \sum_{\ell\in\mathcal{N}'} X_{n\ell}Q_\ell, \quad \forall\, n \in \mathcal{N}'. \tag{10}$$

III. Problem Formulation

In this section we will begin with formulating different components of the cost function for the optimization problem. Next, we will describe the general SOID problem, consider a special case, and also present a distributed version of the problem that promotes scalability.

A. Cost Function

The formulation of the cost function encapsulates a variety of power-quality and customer-oriented objectives. In particular, consider the following functions:

$$\rho(V, I) = \sum_{(m,n)\in\mathcal{E}} \mathrm{Re}\{y^*_{mn}\}\big(\,(\mathrm{Re}\{V_m\} + \mathrm{Re}\{V_n\})^2 + (\mathrm{Im}\{V_m\} + \mathrm{Im}\{V_n\})^2\,\big) \tag{11}$$

$$\phi(P_{\rm c}, Q_{\rm c}) = \sum_{h\in\mathcal{H}} a_h P^2_{{\rm c},h} + b_h P_{{\rm c},h} + c_h Q^2_{{\rm c},h} + d_h|Q_{{\rm c},h}|. \tag{12}$$

$$\nu(V) = \sum_{n\in\mathcal{N}} \left(|V|_n - \frac{1}{N+1}\sum_{\ell\in\mathcal{N}}|V|_\ell\right)^2. \tag{13}$$

Above, ρ denotes the real-power losses in the network; ϕ establishes a quadratic cost on the curtailed active power and generated reactive power and ν attempts to minimize voltage deviations from the average. The choice of a_h , b_h, c_h, and d_h can be based on agreements between customer and utility. Note that the derivation for the expression corresponding to the losses (11) is provided in Appendix A.

B. SOID Problem: General Case

Using the functions defined in (11)-(13), let the overall cost function to be optimized be defined as $C_{\rm opt}$. It follows that:

$$C_{\rm opt}(V, P_{\rm c}, Q_{\rm c}) = c_\rho\rho(V) + c_\phi\phi(P_{\rm c}, Q_{\rm c}) + c_\nu\nu(|V|) \tag{14}$$

and subsequently, the SOID problem is formulated as follows:

$$\min_{V,P_{\rm c},Q_{\rm c}} \; C_{\rm opt}(V,P_{\rm c},Q_{\rm c}) \tag{15a}$$

subject to

$$\begin{aligned}
{\rm Re}\{V_n\} &= 1+\sum_{\ell\in\mathcal{N}'}(R_{n\ell}(P_{{\rm av},\ell}-P_{{\rm c},\ell}-P_{{\rm d},\ell}) \\
&\quad + X_{n\ell}(Q_{{\rm c},\ell}-Q_{{\rm d},\ell})), \qquad \forall\, n\in\mathcal{N}' \qquad (15b)\\
{\rm Im}\{V_n\} &= \sum_{\ell\in\mathcal{N}'}(X_{n\ell}(P_{{\rm av},\ell}-P_{{\rm c},\ell}-P_{{\rm d},\ell}) \\
&\quad - R_{n\ell}(Q_{{\rm c},\ell}-Q_{{\rm d},\ell})), \qquad \forall\, n\in\mathcal{N}' \qquad (15c)\\
V_{\min} &\le 1+\sum_{\ell\in\mathcal{N}'}R_{n\ell}(P_{{\rm av},\ell}-P_{{\rm c},\ell}-P_{{\rm d},\ell}) \\
&\quad + \sum_{\ell\in\mathcal{N}'}X_{n\ell}(Q_{{\rm c},\ell}-Q_{{\rm d},\ell}) \qquad (15d)\\
V_{\max} &\ge 1+\sum_{\ell\in\mathcal{N}'}R_{n\ell}(P_{{\rm av},\ell}-P_{{\rm c},\ell}-P_{{\rm d},\ell}) \\
&\quad + \sum_{\ell\in\mathcal{N}'}X_{n\ell}(Q_{{\rm c},\ell}-Q_{{\rm d},\ell}) \qquad (15e)\\
0 &\le P_{{\rm c},h}\le P_{{\rm av},h} \qquad \forall\, h\in\mathcal{H} \qquad (15f)\\
Q_{{\rm c},h}^2 &\le (S_h^2-(P_{{\rm av},h}-P_{{\rm c},h})^2) \qquad \forall\, h\in\mathcal{H} \qquad (15g)\\
|Q_{{\rm c},h}| &\le \tan\overline{\theta}(P_{{\rm av},h}-P_{{\rm c},h}) \qquad \forall\, h\in\mathcal{H} \qquad (15h)
\end{aligned}$$

Above, (15b)–(15c) capture voltages across the network; (15d)–(15e) force the voltages to stay within defined limits $V_{\min}$ and $V_{\max}$; and (15f)–(15h) defines the set of feasible operating points of each inverter, with $\cos\overline{\theta}$ denoting the minimum allowable power factor.

Note that the problem above is a QCQP in the optimization variables $V, P_{\rm c}, Q_{\rm c}$. Key to ensuring this is the linearized expression for the voltage in (13) and (15b). As such, this QCQP can be solved with lower computational burden compared to semidefinite programming methods, that we previously utilized in our work [6]. Notice further that, by utilizing relations (7)–(8), the cost function and constraints in (15) can be expressed in terms of the powers $P_{\rm c}, Q_{\rm c}$, and the vector-valued variable V can be discarded. Next, we consider a further simplification/approximation that renders the problem to be a Linearly Constrained Quadratic Problem (LCQP).

C. SOID Problem: Special Case

If we consider a resistive network, where we neglect all reactive flows, i.e., $Q_{{\rm c},h}=0$, then the problem in (15) reduces to the following:

$$\min_{P_{\rm c}} \; C_{\rm opt}(P_{\rm c}) \tag{16a}$$

subject to

$$\begin{aligned}
V_{\min} &\le 1+\sum_{\ell\in\mathcal{N}'}R_{n\ell}P_{\ell} \qquad (16b)\\
V_{\max} &\ge 1+\sum_{\ell\in\mathcal{N}'}R_{n\ell}P_{\ell}, \qquad \forall\, n\in\mathcal{N}' \qquad (16c)\\
0 &\le P_{{\rm c},h}\le P_{{\rm av},h}, \qquad \forall\, h\in\mathcal{H}. \qquad (16d)
\end{aligned}$$

The absence of (15g)–(15h) in this formulation, renders this problem formulation a LCQP. Although the problems described here and in the previous section are computationally affordable, distributed implementations leveraging the alternate direction method of multipliers are presented next to facilitate scalability to large distribution networks with limited information exchanges.

D. Distributed Implementation Leveraging ADMM

The main motivation for the development of a distributed solver for (15) is to enable utility and customers to pursue specific optimization objectives, while ensuring that system-level power-flow and voltage-regulation constraints are satisfied. To this end, the ADMM is leveraged next to decouple utility- and customer-orientated objectives and constraints. Utility optimization includes minimizing power losses in the network and correcting voltage deviations. Customer based optimization includes minimizing the cost incurred in active power curtailment.

To this end, key is to introduce auxiliary vector-valued variables $\widetilde{P}$ and $\widetilde{Q}$ that represent copies of the inverter setpoints P and Q on the utility side. Using these new variables in the cost function in (14), the optimization problem (15) can be reformulated in the following equivalent way:

$$\min_{\substack{V,\{P_{{\rm c},h},Q_{{\rm c},h}\}\\ \{\widetilde{P}_h,\widetilde{Q}_h\}}} \; C_{\rm u}(V,\widetilde{P},\widetilde{Q})+\sum_{\ell\in\mathcal{H}}C_{{\rm c},\ell}(P_{{\rm c},\ell},Q_{{\rm c},\ell})$$

subject to (15f) − (15h) and

$$\begin{aligned}
{\rm Re}\{V_n\} &= 1+\sum_{\ell\in\mathcal{N}'}(R_{n\ell}\widetilde{P}_{\ell}+X_{n\ell}\widetilde{Q}_{\ell}) \qquad (17a)\\
{\rm Im}\{V_n\} &= \sum_{\ell\in\mathcal{N}'}(X_{n\ell}\widetilde{P}_{\ell}-R_{n\ell}\widetilde{Q}_{\ell}) \qquad (17b)\\
V_{\min} &\le 1+\sum_{\ell\in\mathcal{N}'}R_{n\ell}\widetilde{P}_{\ell}+\sum_{\ell\in\mathcal{N}'}X_{n\ell}\widetilde{Q}_{\ell}\\
V_{\max} &\ge 1+\sum_{\ell\in\mathcal{N}'}R_{n\ell}\widetilde{P}_{\ell}+\sum_{\ell\in\mathcal{N}'}X_{n\ell}\widetilde{Q}_{\ell}, \quad \forall\, n\in\mathcal{N}'\\
\widetilde{P}_h &= P_{{\rm av},h}-P_{{\rm c},h}-P_{{\rm d},h} \qquad \forall\, h\in\mathcal{H} \qquad (17c)\\
\widetilde{Q}_h &= Q_{{\rm c},h}-Q_{{\rm d},h}, \qquad \forall\, h\in\mathcal{H}. \qquad (17d)
\end{aligned}$$

The next steps involve the introduction of auxiliary variables to facilitate the decomposability of the constraints (17c) and (17d) across utility and inverters, and the partition of the linearized voltage expressions (17a) and (17b) into two groups: nodes with and without PV systems. Utility-related optimization variables, V, $\widetilde{P}$, and $\widetilde{Q}$, are collected in the set $\mathcal{O}:=\{V,\widetilde{P},\widetilde{Q}\}$. Customer-related decision variables, $P_{\rm c}$, $Q_{\rm c}$, are collected in the set $\mathcal{P}_h:=\{P_{{\rm c},h},Q_{{\rm c},h},\forall h\in\mathcal{H}\}$ and $\mathcal{P}_{xy}:=\{x_h,y_h,\forall h\in\mathcal{H}\}$ denotes the set that collects the auxiliary variables. Dual variables are collected in the set $\mathcal{D}:=\{\overline{\lambda}_h,\lambda_h,\overline{\mu}_h,\mu_h,\forall h\in\mathcal{H}\}$; and $\kappa>0$ is a given constant. Finally, $\mathcal{L}_u(\mathcal{O})$ and $\mathcal{L}_h(\mathcal{P}_h)$ denote the partial Lagrangian functions for the utility and customer side respectively, and they are spelled out in (24) and (25), respectively. Then, following the procedure provided in Appendix B and leveraging ADMM [22, Sec. 3.4], it can be shown that the distributed algorithm boils down to the steps **[S1]-[S2]**

performed iteratively as described below (m represent the iteration index):

[S1a] Variables $V[m+1], \widetilde{P}_h[m+1], \widetilde{Q}_h[m+1]$ are updated as:

$$\mathcal{O} := \arg \min_{V,\{\widetilde{P},\widetilde{Q}\}} \mathcal{L}_u(V, \widetilde{P}, \widetilde{Q}) \tag{18}$$

$$\text{subject to (22b)} - \text{(22c) and}$$

$$V_{\min} \leq 1 + \sum_{\ell \in \mathcal{N}'} R_{n\ell} \widetilde{P}_\ell + \sum_{\ell \in \mathcal{N}'} X_{n\ell} \widetilde{Q}_\ell$$

$$V_{\max} \geq 1 + \sum_{\ell \in \mathcal{N}'} R_{n\ell} \widetilde{P}_\ell + \sum_{\ell \in \mathcal{N}'} X_{n\ell} \widetilde{Q}_\ell, \quad \forall\, n \in \mathcal{N}'$$

[S1b] Variables $P_{\mathrm{c},h}[m+1], Q_{\mathrm{c},h}[m+1]$ are updated as:

$$\mathcal{P}_h := \arg \min_{\{P_{\mathrm{c}}, Q_{\mathrm{c}}\}} \mathcal{L}_h(P_{\mathrm{c}}, Q_{\mathrm{c}}) \tag{19}$$

$$\begin{aligned} \text{s.to} \quad & 0 \leq P_{\mathrm{c},h} \leq P_{\mathrm{av},h} \\ & Q_{\mathrm{c},h}^2 \leq (S_h^2 - (P_{\mathrm{av},h} - P_{\mathrm{c},h})^2) \\ & |Q_{\mathrm{c},h}| \leq \tan\overline{\theta}(P_{\mathrm{av},h} - P_{\mathrm{c},h}) \ , \forall h \in \mathcal{H} \end{aligned}$$

[S2] Dual variables are updated as follows:

$$\begin{aligned} \lambda_h[m+1] = \lambda_h[m] + \frac{\kappa}{2}(\widetilde{P}_h[m+1] - P_{\mathrm{av},h} + P_{\mathrm{d},h} \\ + P_{\mathrm{c},h}[m+1]) \end{aligned} \tag{20a}$$

$$\begin{aligned} \mu_h[m+1] = \mu_h[m] + \frac{\kappa}{2}(\widetilde{Q}_h[m+1] + Q_{\mathrm{d},h} \\ - Q_{\mathrm{c},h}[m+1]). \end{aligned} \tag{20b}$$

To implement the above algorithm, we require two-way communication of the values $\overline{P}_c[m], \overline{Q}_s[m]$ and $\widetilde{P}_c[m], \widetilde{Q}_s[m]$ between utility and customers. For every iteration $m > 0$, (18) is solved on utility side to update the variables in the set $\mathcal{O}$. Eventually PV-inverter setpoints satisfying power quality objectives are obtained. Simultaneously customer side PV-inverter setpoints are updated via (19) and subsequently sent to the utility. Once these set points are exchanged, dual variables are updated at utility and customers, respectively through (20). While the problem setup considered here is different from that in [27], convergence of the algorithm described above to the solution of (15) can be shown leveraging [27, *Proposition 1*]. Finally, once the distributed algorithm is converged, all the PV-inverter set points are implemented at the PV inverters.

Algorithm 1 Distributed Scheme

Set $\lambda_h[0] = \mu_h[0] = 0$ for all $h \in \mathcal{H}$.
for $m = 1, 2, \ldots$ (repeat until convergence) **do**
1. **[Utility]**: update $\mathcal{O}[m+1]$ via (18).
   [Customer-h]: update $\mathcal{P}_h[m+1]$ via (19).
2. **[Utility]**: send $\mathcal{O}[m+1] \setminus |V|[m+1]$ to Customer;
   repeat for all $h \in \mathcal{H}$.
   [Customer-h]: receive $\mathcal{O}[m+1] \setminus |V|[m+1]$ from utility;
   send $\mathcal{P}_h[m+1]$ to utility;
   repeat for all $h \in \mathcal{H}$.
   [Utility]: receive $\mathcal{P}_h[m+1]$ from Customer;
   repeat for all $h \in \mathcal{H}$.
3. **[Utility]**: update $\{\lambda_h[m+1], \mu_h[m+1]\}_{h \in \mathcal{H}}$ via (20).
   [Customer-h]: update $\lambda_h[m+1], \mu_h[m+1]$ via (20);
   repeat for all $h \in \mathcal{H}$.

end for
Implement real and reactive setpoints in the PV inverters.

IV. Numerical Case Studies

We consider suitably modified versions of the IEEE 2500- and IEEE 123-node test feeders for the case studies. In particular, the IEEE 2500- and IEEE 123-node systems are used to discuss voltage profile across nodes using various renditions of the SOID strategies; while simulation results for the IEEE 123-node system help us to compare the accuracy with respect to SDP-based optimization methods in [6]. For all simulations, it is assumed that the network admittance matrix Y, available power P_{av}, load demand P_{d}, Q_{d} and inverter ratings S are known. Voltage limits $V_{\min}$ and $V_{\max}$ are set to 0.917 and 1.042 p.u. respectively [1]. The optimization package CVX [28] as part of MATLAB is used to run SOID and the distributed problem formulations proposed in this paper. Dc-ac derating coefficient for the PV systems is set to 0.77 [29]. Three different kind of dc ratings (5.52kW, 5.7kW and 9kW) have been used [30], [31]; and the PV inverters are oversized by 10% of resultant ac rating [4]. The minimum power factor of inverters is set to 0.85 [32]. System Advisory Model provided by NREL is used to compute active powers available during the day. Open Energy Info Database was used to obtain the load profile. For the simulations, the base load experienced in Saint Paul, MN, USA, during the month of July is utilized. All the plots are in accordance with the data considered during day time at 14:00. Finally, the voltage at the secondary of the step-down transformer (considered as slack bus in the model) is set to 1.02 p.u.

A. Accuracy of Linear Approximation

To demonstrate the accuracy of the linear approximation compared to the original nonlinear power-flow equations, we plot in Fig. 2 voltage magnitude and phase angles recovered from the linear power-flow approximation and those obtained

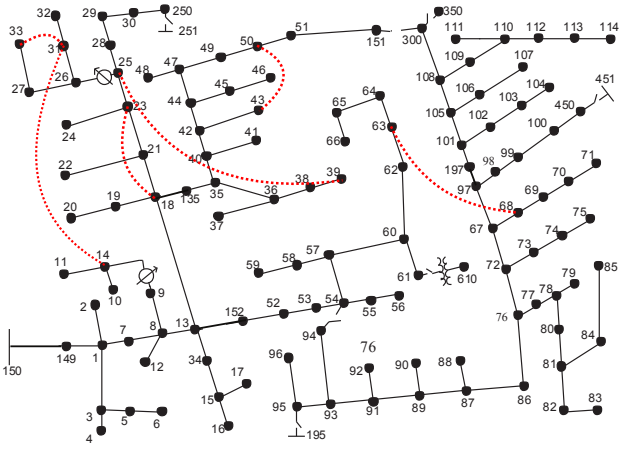

Fig. 1. IEEE 123-node distribution feeder with PV systems assumed to be present at nodes: 2, 4, 6, 10, 11, 12, 16, 17, 19, 20, 22, 24, 27, 32, 33, 36, 37, 38, 39, 41, 43, 46, 48, 49, 50, 51, 56, 59, 65, 66, 71, 75, 79, 83, 85, 88, 90, 92, 94, 96, 104, 107, 111, 114, 151, 250, 300, 450. Lines in dashed red indicate the modified meshed network that is also utilized in the case studies.

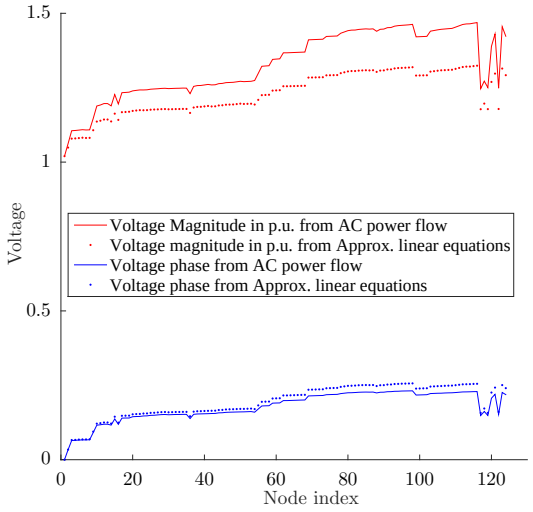

Fig. 2. Accuracy of linear approximation.

from the solution of the nonlinear power-flow equations (following [6]) for the IEEE 123-node test feeder system depicted in Fig. 1. By and large, we see that errors are minimal; congruently problems formulated in Section III-B using this linear approximation offer computational speedup of up to 75%, which we further comment on in the next section. In Fig. 2, nodes with higher numbering are, in general, electrically more distant from the reference bus. Consequently, we see that errors increase as we move electrically further away from the reference bus. Nonetheless, it is worth mentioning that the errors conform to the bounds in [13], [14].

B. SOID Plots for Different Cases

Results for the IEEE 2500-node test feeder system are plotted in Fig. 3 and for the IEEE 123-node test-feeder system in Fig. 4 and Fig. 5. Results for the modified IEEE 123-node meshed network are plotted in Fig. 6. IEEE 123-node meshed network is obtained from suitably modifying the test feeder system by introducing lines as indicated by red dotted lines in Fig. 1. It should be noted that these voltage plots correspond to the nonlinear AC simulation of the original power flow equations. It can be seen that if no control strategy is implemented, then the upper voltage limit (plotted as a flat cyan line) is violated due to increased loading of the system. We implement two different cases, SOID-A1 and SOID-A2, with respect to the cost function in (14). Optimization parameters for strategy SOID-A1 are $c_\rho = 1$, $c_\phi = 1$, $c_\nu = 0$, $a_h = 0.1, b_h = c_h = d_h = 0$ (and results are plotted in red); for strategy SOID-A2, we penalize voltage deviations from the average by setting $c_\rho = 1$, $c_\phi = 1$, $c_\nu = 1$, $a_h = 0.1, b_h = c_h = d_h = 0$ (and results are plotted in dark blue). In Fig. 3, given space limits, we plot only the voltages for the first 100 nodes to demonstrate that the system is operating at prescribed limits. The average computational time required to solve the problem formulated in Section III-B for IEEE 2500-node system was 600 sec; the computation times for the different cases corresponding to the IEEE 123-node system are tabulated in Table I. (Note that the computational time is calculated with reference to time when no control strategy is implemented and hence, the first row of the table contains 0's.) The computation times for the meshed network are not reported, since they are approximately the same as those in Table I. This table also provides a comparison with the OID framework setup proposed in [6]. The simulation was run on a machine with an Intel core i7-4710HQ CPU @ 2.5 GHz. It can be seen that as we progress by adding objective terms one at a time to the cost function from 'No Control Strategy' to 'SOID-A2', the average computational time increases.

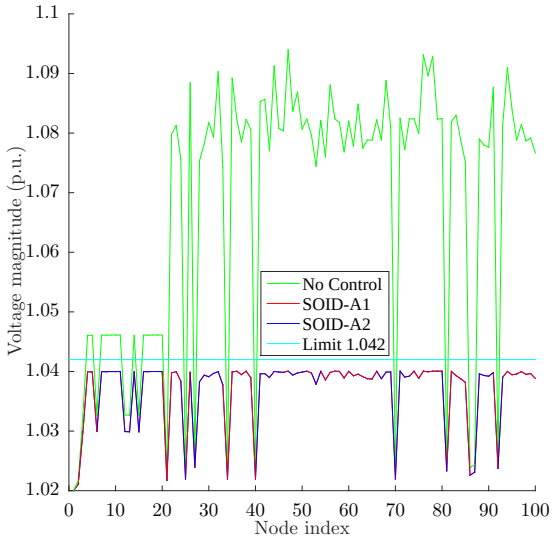

Fig. 3. Voltage profile across nodes in the network for SOID formulated in Section III-B for IEEE 2500-node system with radial structure.

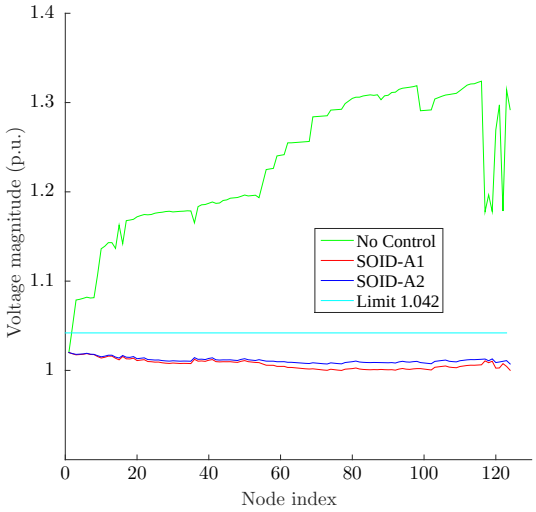

Fig. 4. Voltage profile across nodes in the network for SOID formulated in Section III-B for IEEE 123-node system with radial structure.

TABLE I
AVERAGE COMPUTATIONAL TIME IN (sec) FOR IEEE 123-NODE TEST FEEDER SYSTEM

Cases in Fig. 4	SOID in Section III-B	SDP-OID
No Control	0	0
SOID - A1	2.01	34.7
SOID - A2	2.51	54.07

C. Convergence of the Distributed Algorithm

Parameters to analyze convergence of the distributed scheme are set as follows: $a_h = 0.1$ and $b_h = 0$. The ADMM constant κ is set equal to 5. Solar irradiance conditions at 14:00 are utilized for this particular case. Figure 7 depicts the trajectories of the iterates $\{\widetilde{P}_h[m]\}_{h\in\mathcal{H}}$ (solid lines) and $\{P_h[m]\}_{h\in\mathcal{H}}$ (dashed lines) for a certain set of selected houses among $\mathrm{H}_1 - \mathrm{H}_{48}$. Finally, the trajectories of error tracking differences between $|\widetilde{P}_h[m] - P_h[m]|$, as a function of the ADMM iteration index are depicted in Fig. 8. It can be clearly seen that the algorithm converges to a set-point that is optimal to both the utility and customers.

V. CONCLUDING REMARKS AND DIRECTIONS FOR FUTURE WORK

This paper developed a suite of scalable algorithms to determine the active- and reactive-power set points for photovoltaic (PV) inverters in residential distribution networks. A linear expression for the voltages expressed in rectangular coordinates was leveraged to get around the non-convexity that would otherwise be encountered in the AC-OPF setting. First, we formulated a quadratic constrained quadratic program (QCQP) by leveraging a linear approximation of the algebraic power-flow equations that ensures optimization of inverter dispatch (quantified, e.g., through power losses, correcting voltage deviations). This was then reduced to a LCQP for resistive dominant networks. A distributed scheme was also proposed to promote scalability and further reduce the computational burden of the optimization problem. Added advantage of the distributed algorithm is that it outlines avenues for the formulation and operation of distribution-network markets. The merits of the proposed approach were demonstrated using a comprehensive set of simulation results that utilized real-world PV-generation and load-profile data for an illustrative low-voltage residential distribution system.

As part of future work, the proposed SOID problems and the distributed versions will be implemented in hardware setups using micro-controllers and a suitable communication medium. We will also study communication-related issues, as well as further simplifications of the optimization problem to make it suitable for practical implementation. An example of such a simplification would be to express the operating region of the PV inverters entirely with linear constraints. Additionally, we will also focus on adopting the approaches suggested in this work for unbalanced multi-phase networks. Also, we will compare the results for the problems (and distributed implementations) with approaches such as SOCP and belief propagation.

VI. APPENDIX

A. Expression for Power Losses in (11)

Begin by expressing the voltage at the m node in the network as $V_m = \mathrm{Re}\{V_m\} + \mathrm{j}\,\mathrm{Im}\{V_m\}$. The expression in (11) can be derived as follows:

$$\begin{aligned}\rho(V,I) &= \sum_{(m,n)\in\mathcal{E}} \mathrm{Re}\{V_m I^*_{(m,n)}\} - \mathrm{Re}\{V_n I^*_{(m,n)}\} \\ &= \sum_{(m,n)\in\mathcal{E}} \mathrm{Re}\{V_m(V_m^* - V_n^*)y_{mn}^*\} - \\ &\qquad \mathrm{Re}\{V_n(V_m^* - V_n^*)y_{mn}^*\} \\ &= \sum_{(m,n)\in\mathcal{E}} \mathrm{Re}\{(V_m(V_m^* - V_n^*) - V_n(V_m^* - V_n^*))y_{mn}^*\}.\end{aligned}$$

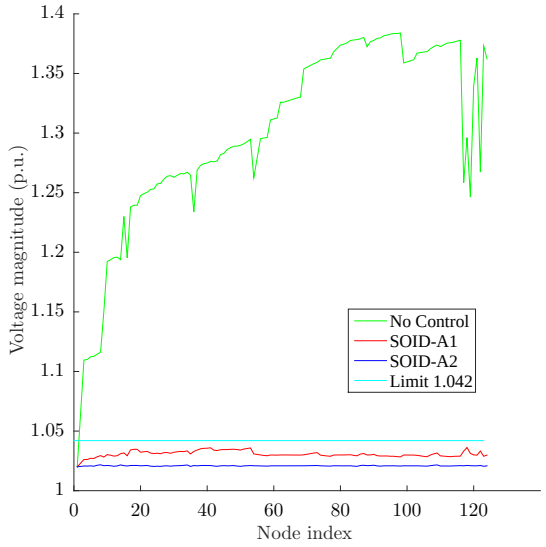

Fig. 5. Voltage profile across nodes in the network for SOID formulated in Section III-C for IEEE 123-node system with radial structure.

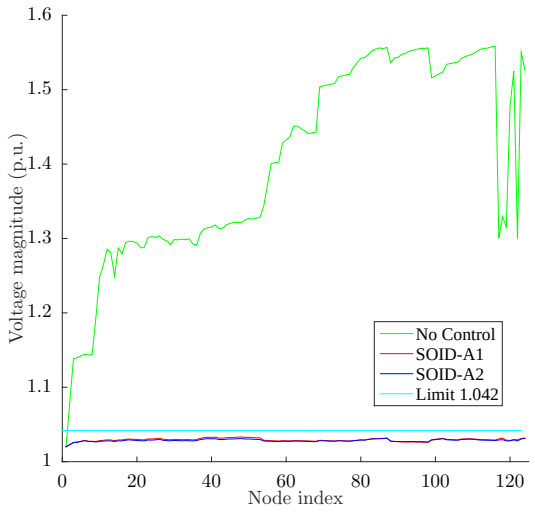

Fig. 6. Voltage profile across nodes in the network for SOID formulated in Section III-B for IEEE 123-node system with mesh structure.

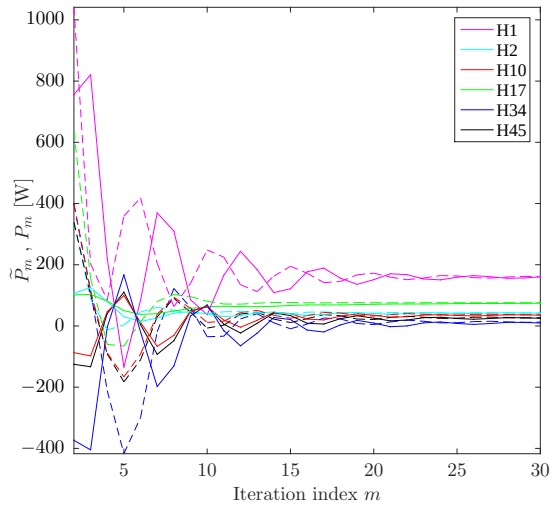

Fig. 7. Convergence of the distributed algorithm.

Expanding the expression above with the rectangular-form adopted for the nodal voltages, we get:

$$\rho(V,I) = \sum_{(m,n)\in\mathcal{E}} \mathrm{Re}\{y^*_{mn}\}\big((\mathrm{Re}\{V_m\} + \mathrm{Re}\{V_n\})^2 + (\mathrm{Im}\{V_m\} + \mathrm{Im}\{V_n\})^2 \big). \tag{21}$$

Other loss modeling methods have been proposed in the literature and could potentially be applied to similar problem settings, one example is [11].

B. Derivation of the ADMM-based Distributed Algorithm

Beginning with (17), the standard procedure it to dualize constraints (17c) and (17d), and subsequently leverage the decomposability of the associated Lagrangian function. However, to favor decomposability of quadratically augmented Lagrangian functions [22, Sec. 3.4], consider first introducing auxiliary variables x_h, y_h and reformulating (17) in the following equivalent way:

$$\min_{\substack{V,\{P_{\mathrm{c},h},Q_{\mathrm{c},h}\}\\ \{\widetilde{P},\widetilde{Q},x_h,y_h\}}} \; C_{\mathrm{u}}(V,\widetilde{P},\widetilde{Q}) + \sum_{\ell\in\mathcal{H}} C_{\mathrm{c},\ell}(P_{\mathrm{c},\ell},Q_{\mathrm{c},\ell}) \tag{22a}$$

$$\text{subject to (15f)} - \text{(15h) and}$$

$$\mathrm{Re}\{V_n\} = 1 + \sum_{\ell\in\mathcal{H}}(R_{n\ell}\widetilde{P}_\ell + X_{n\ell}\widetilde{Q}_\ell) - \sum_{\ell\in\mathcal{N}'\setminus\mathcal{H}}(R_{n\ell}P_{\mathrm{d},\ell} + X_{n\ell}Q_{\mathrm{d},\ell}) \quad \forall\, n\in\mathcal{N}' \tag{22b}$$

$$\mathrm{Im}\{V_n\} = \sum_{\ell\in\mathcal{H}}(X_{n\ell}\widetilde{P}_\ell - R_{n\ell}\widetilde{Q}_\ell) - \sum_{\ell\in\mathcal{N}'\setminus\mathcal{H}}(X_{n\ell}P_{\mathrm{d},\ell} - R_{n\ell}Q_{\mathrm{d},\ell}) \quad \forall\, n\in\mathcal{N}' \tag{22c}$$

$$V_{\min} \le 1 + \sum_{\ell\in\mathcal{N}'} R_{n\ell}\widetilde{P}_\ell + \sum_{\ell\in\mathcal{N}'} X_{n\ell}\widetilde{Q}_\ell$$

$$V_{\max} \ge 1 + \sum_{\ell\in\mathcal{N}'} R_{n\ell}\widetilde{P}_\ell + \sum_{\ell\in\mathcal{N}'} X_{n\ell}\widetilde{Q}_\ell, \quad \forall\, n\in\mathcal{N}'$$

$$\widetilde{P}_h = x_h \qquad \forall\, h\in\mathcal{H} \tag{22d}$$

$$x_h = P_{\mathrm{av},h} - P_{\mathrm{d},h} - P_{\mathrm{c},h} \qquad \forall\, h\in\mathcal{H} \tag{22e}$$

$$\widetilde{Q}_h = y_h \qquad \forall\, h\in\mathcal{H} \tag{22f}$$

$$y_h = -Q_{\mathrm{d},h} + Q_{\mathrm{c},h}, \qquad \forall\, h\in\mathcal{H}. \tag{22g}$$

Now, (22) can be solved in a distributed fashion by dualizing constraints (22d)–(22g) and leveraging ADMM [22, Sec. 3.4]. To this end, let $\lambda_h, \overline{\lambda}_h, \mu_h, \overline{\mu}_h$ be the Lagrange multipliers associated with (22d)–(22g), where h is the inverter index. Then the quadratically augmented Lagrangian can be obtained as:

$$\begin{aligned}\mathcal{L}(\mathcal{O},\mathcal{P}_h,\mathcal{P}_{xy},\mathcal{D}) &:= C_{\mathrm{u}}(V,\widetilde{P},\widetilde{Q}) + \sum_{\ell\in\mathcal{H}} C_{\mathrm{c},\ell}(P_{\mathrm{c},\ell},Q_{\mathrm{c},\ell})\\ &+ \sum_{h\in\mathcal{H}}\Big(\lambda_h(\widetilde{P}_h - x_h) + \overline{\lambda}_h(x_h - P_{\mathrm{av},h} + P_{\mathrm{d},h} + P_{\mathrm{c},h})\Big)\\ &+ \sum_{h\in\mathcal{H}}\Big(\mu_h(\widetilde{Q}_h - y_h) + \overline{\mu}_h(y_h + Q_{\mathrm{d},h} - Q_{\mathrm{c},h})\Big)\\ &+ \sum_{h\in\mathcal{H}}\Big(\frac{\kappa}{2}(\widetilde{P}_h - x_h)^2 + \frac{\kappa}{2}(x_h - P_{\mathrm{av},h} + P_{\mathrm{d},h} + P_{\mathrm{c},h})^2\Big)\\ &+ \sum_{h\in\mathcal{H}}\Big(\frac{\kappa}{2}(\widetilde{Q}_h - y_h)^2 + \frac{\kappa}{2}(y_h + Q_{\mathrm{d},h} - Q_{\mathrm{c},h})^2\Big)\end{aligned} \tag{23}$$

where utility related optimization variables are collected in $\mathcal{O} := \{V,\widetilde{P},\widetilde{Q}\}$; Customer related decision variables are collected in $\mathcal{P}_h := \{P_{\mathrm{c},h}, Q_{\mathrm{c},h}, \forall h\in\mathcal{H}\}$; $\mathcal{P}_{xy} := \{x_h, y_h, \forall h\in\mathcal{H}\}$ is the set of auxiliary variables; Dual variables are collected in $\mathcal{D} := \{\overline{\lambda}_h, \lambda_h, \overline{\mu}_h, \mu_h, \forall h\in\mathcal{H}\}$; and $\kappa > 0$ is a given constant. Using [27, *Lemma 1*] and (23) we can define individual partial Lagrangian functions for utility as $\mathcal{L}_u(\mathcal{O})$

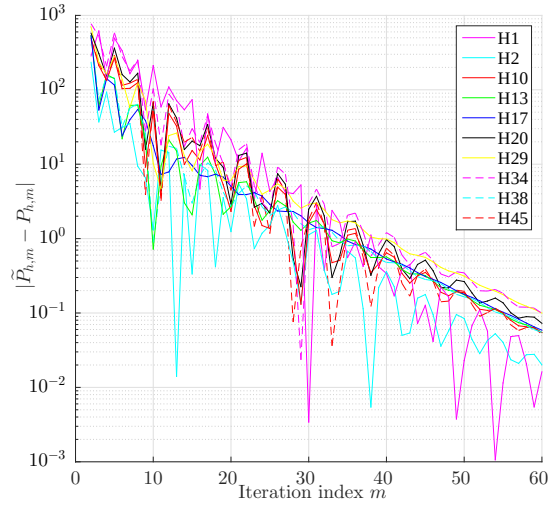

Fig. 8. Error plot for power curtailment

and customer side as $\mathcal{L}_h(\mathcal{P}_h)$ for the mth iteration as below:

$$\mathcal{L}_u(\mathcal{O}) := C_{\rm u}(V,\widetilde{P},\widetilde{Q}) + \sum_{h\in\mathcal{H}} \frac{\kappa}{2}(\widetilde{P}^2+\widetilde{Q}^2) + \sum_{h\in\mathcal{H}} \widetilde{P}_h\Big(\lambda_h[m] - \frac{\kappa}{2}(\widetilde{P}_h[m] + P_{{\rm av},h} - P_{{\rm d},h} - P_{{\rm c},h}[m])\Big) + \sum_{h\in\mathcal{H}} \widetilde{Q}_h\Big(\mu_h[m] - \frac{\kappa}{2}(\widetilde{Q}_h[m] - Q_{{\rm d},h} + Q_{{\rm c},h}[m])\Big) \quad (24)$$

$$\mathcal{L}_h(\mathcal{P}_h) := C_{c,h}(P_{{\rm c},h},Q_{{\rm c},h}) + \sum_{h\in\mathcal{H}} \frac{\kappa}{2}(P_{{\rm c},h}^2+Q_{{\rm c},h}^2) + P_{{\rm c},h}\Big(\lambda_h[m] - \frac{\kappa}{2}(-P_{{\rm c},h}[m] - P_{{\rm av},h} + P_{{\rm d},h} - \widetilde{P}_h[m])\Big) + Q_{{\rm c},h}\Big(-\mu_h[m] - \frac{\kappa}{2}(\widetilde{Q}_h[m] + Q_{{\rm d},h} + Q_{{\rm c},h}[m])\Big). \quad (25)$$

By minimizing the respective partial Lagrangian function at the utility and inverter sides, one obtains steps [S1]–[S2]. It is also worth mentioning that various techniques have been proposed in the literature to select the value of κ with a view towards improving convergence, see, e.g., [33], [34].

REFERENCES

[1] R. Tonkoski, L. A. Lopes, and T. H. El-Fouly, "Coordinated active power curtailment of grid connected pv inverters for overvoltage prevention," *Sustainable Energy, IEEE Transactions on*, vol. 2, no. 2, pp. 139–147, 2011.

[2] A. Samadi, R. Eriksson, L. Soder, B. G. Rawn, and J. C. Boemer, "Coordinated active power-dependent voltage regulation in distribution grids with pv systems," *Power Delivery, IEEE Transactions on*, vol. 29, no. 3, pp. 1454–1464, 2014.

[3] P. Jahangiri and D. C. Aliprantis, "Distributed volt/var control by pv inverters," *Power Systems, IEEE Transactions on*, vol. 28, no. 3, pp. 3429–3439, 2013.

[4] K. Turitsyn, P. Sulc, S. Backhaus, and M. Chertkov, "Options for control of reactive power by distributed photovoltaic generators," *Proceedings of the IEEE*, vol. 99, no. 6, pp. 1063–1073, 2011.

[5] A. Cagnano, E. De Tuglie, M. Liserre, and R. A. Mastromauro, "Online optimal reactive power control strategy of pv inverters," *Industrial Electronics, IEEE Transactions on*, vol. 58, no. 10, pp. 4549–4558, 2011.

[6] E. Dall'Anese, S. V. Dhople, and G. B. Giannakis, "Optimal dispatch of photovoltaic inverters in residential distribution systems," *Sustainable Energy, IEEE Transactions on*, vol. 5, no. 2, pp. 487–497, 2014.

[7] J. Lavaei and S. H. Low, "Zero duality gap in optimal power flow problem," *Power Systems, IEEE Transactions on*, vol. 27, no. 1, pp. 92–107, 2012.

[8] Y. Nesterov, A. Nemirovskii, and Y. Ye, *Interior-point polynomial algorithms in convex programming*. SIAM, 1994, vol. 13.

[9] E. De Klerk, "Exploiting special structure in semidefinite programming: A survey of theory and applications," *European Journal of Operational Research*, vol. 201, no. 1, pp. 1–10, 2010.

[10] R. Madani, M. Ashraphijuo, and J. Lavaei, "Promises of conic relaxation for contingency-constrained optimal power flow problem," *IEEE Transactions on Power Systews*, vol. 31, no. 2, pp. 1297–1307, March 2015.

[11] R. Jabr, "Radial distribution load flow using conic programming," *IEEE Transactions on Power Systems*, vol. 21, no. 3, pp. 1458–1459, 2006.

[12] C. Coffrin, H. L. Hijazi, and P. Van Hentenryck, "The QC Relaxation: Theoretical and Computational Results on Optimal Power Flow," *arXiv preprint arXiv:1502.07847*, 2015.

[13] S. Bolognani and S. Zampieri, "On the existence and linear approximation of the power flow solution in power distribution networks," *IEEE Transactions on Power Systems*, vol. 31, no. 1, pp. 163–172, January 2016.

[14] S. V. Dhople, S. S. Guggilam, and Y. C. Chen, "Linear approximations to AC power flow in rectangular coordinates," 2015. [Online]. Available: http://arxiv.org/abs/1512.06903

[15] J. de Hoog, T. Alpcan, M. Brazil, D. A. Thomas, and I. Mareels, "Optimal charging of electric vehicles taking distribution network constraints into account," *Power Systems, IEEE Transactions on*, vol. 30, no. 1, pp. 365–375, 2015.

[16] A. J. Wood and B. F. Wollenberg, *Power generation, operation, and control*. John Wiley & Sons, 2012.

[17] L. Gan and S. H. Low, "Convex relaxations and linear approximation for optimal power flow in multiphase radial networks," in *Power Systems Computation Conference (PSCC), 2014*. IEEE, 2014, pp. 1–9.

[18] M. C. Richard P O'Neill, Anya Castillo, "The IV formulation and linear approximations of the ac optimal power flow problem," 2012. [Online]. Available: https://www.ferc.gov/industries/electric/indus-act/market-planning/opf-papers/acopf-2-iv-linearization.pdf

[19] H. Zhang, V. Vittal, G. T. Heydt, and J. Quintero, "A relaxed AC optimal power flow model based on a taylor series," in *Innovative Smart Grid Technologies-Asia (ISGT Asia), 2013 IEEE*. IEEE, 2013, pp. 1–5.

[20] A. M. Koster and S. Lemkens, "Designing AC power grids using integer linear programming," in *Network Optimization*. Springer, 2011, pp. 478–483.

[21] E. Dall'Anese, S. V. Dhople, and G. B. Giannakis, "Photovoltaic inverter controllers seeking AC optimal power flow solutions," *arXiv preprint arXiv:1501.00188*, 2014.

[22] D. P. Bertsekas and J. N. Tsitsiklis, *Parallel and distributed computation: numerical methods*. Prentice-Hall, Inc., 1989.

[23] S. Boyd, N. Parikh, E. Chu, B. Peleato, and J. Eckstein, "Distributed optimization and statistical learning via the alternating direction method of multipliers," *Foundations and Trends in Machine Learning*, vol. 3, no. 1, pp. 1–122, 2011.

[24] P. Scott and S. Thiebaux, "Distributed multi-period optimal power flow for demand response in microgrids," in *Proceedings of the 2015 ACM Sixth International Conference on Future Energy Systems*. ACM, 2015, pp. 17–26.

[25] P. Sulc, S. Backhaus, and M. Chertkov, "Optimal distributed control of reactive power via the alternating direction method of multipliers," *Energy Conversion, IEEE Transactions on*, vol. 29, no. 4, pp. 968–977, 2014.

[26] T. Erseghe, D. Zennaro, E. Dall'Anese, and L. Vangelista, "Fast consensus by the alternating direction multipliers method," *Signal Processing, IEEE Transactions on*, vol. 59, no. 11, pp. 5523–5537, 2011.

[27] E. Dall'Anese, S. V. Dhople, B. B. Johnson, and G. Giannakis, "Decentralized optimal dispatch of photovoltaic inverters in residential distribution systems," *Energy Conversion, IEEE Transactions on*, vol. 29, no. 4, pp. 957–967, 2014.

[28] M. Grant, S. Boyd, and Y. Ye, "CVX: Matlab software for disciplined convex programming," 2008.

[29] D. L. King, S. Gonzalez, G. M. Galbraith, and W. E. Boyson, "Performance model for grid-connected photovoltaic inverters."

[30] S. T. Cady, D. Mestas, and C. Cirone, "Engineering systems in the re_home: A net-zero, solar-powered house for the US department of energy's 2011 solar decathlon," in *Power and Energy Conference at Illinois (PECI), 2012 IEEE*. IEEE, 2012, pp. 1–5.

[31] S. V. Dhople, J. L. Ehlmann, C. J. Murray, S. T. Cady, and P. L. Chapman, "Engineering systems in the gable home: A passive, net-zero, solar-powered house for the U.S. department of energy's 2009 solar decathlon," in *Power and Energy Conference at Illinois (PECI), 2010*. IEEE, 2010, pp. 58–62.

[32] T. Stetz, J. Künschner, M. Braun, and B. Engel, "Cost-optimal sizing of photovoltaic inverters–influence of new grid codes and cost reductions," in *25th European PV Solar Energy Conference and Exhibition. Valencia*, 2010.

[33] E. Ghadimi, A. Teixeira, I. Shames, and M. Johansson, "Optimal parameter selection for the alternating direction method of multipliers (ADMM): quadratic problems," *Automatic Control, IEEE Transactions on*, vol. 60, no. 3, pp. 644–658, 2015.

[34] A. U. Raghunathan and S. Di Cairano, "Optimal step-size selection in alternating direction method of multipliers for convex quadratic programs and model predictive control,," in *Proceedings of Symposium on Mathematical Theory of Networks and Systems*, 2014, pp. 807–814.

Swaroop S. Guggilam (S'15) received the Bachelor's degree in electrical engineering from the Veermata Jijabai Technological Institute, Mumbai, Maharashtra, India, in 2013 and M.S. degree in electrical engineering from the University of Minnesota, Minneapolis, MN, USA, in 2015. He is currently working toward the Ph.D. degree in electrical engineering from the University of Minnesota, Minneapolis, MN, USA.

His research interests include distribution networks, optimization, power system modeling, analysis and control for increasing renewable integration.

Emiliano Dall'Anese (S'08–M'11) received the Laurea Triennale (B.Sc Degree) and the Laurea Specialistica (M.Sc Degree) in Telecommunications Engineering from the University of Padova, Italy, in 2005 and 2007, respectively, and the Ph.D. in Information Engineering from the Department of Information Engineering, University of Padova, Italy, in 2011. From January 2009 to September 2010, he was a visiting scholar at the Department of Electrical and Computer Engineering, University of Minnesota, USA. From January 2011 to November 2014 he was a Postdoctoral Associate at the Department of Electrical and Computer Engineering and Digital Technology Center of the University of Minnesota, USA. Since December 2014 he has been a Senior Engineer at the National Renewable Energy Laboratory, Golden, CO, USA.

His current research focuses on distributed optimization and control of power distribution networks with distributed energy resources and statistical inference for data analytics.

Yu Christine Chen (S'10–M'15) received the B.A.Sc. degree in engineering science from the University of Toronto, Toronto, ON, Canada, in 2009, and the M.S. and Ph.D. degrees in electrical engineering from the University of Illinois at Urbana-Champaign, Urbana, IL, USA, in 2011 and 2014, respectively.

She is currently an Assistant Professor with the Department of Electrical and Computer Engineering, The University of British Columbia, Vancouver, BC, Canada, where she is affiliated with the Electric Power and Energy Systems Group. Her research interests include power system analysis, monitoring, and control.

Sairaj V. Dhople (S'09–M'13) received the B.S., M.S., and Ph.D. degrees in electrical engineering, in 2007, 2009, and 2012, respectively, from the University of Illinois, Urbana-Champaign. He is currently an Assistant Professor in the Department of Electrical and Computer Engineering at the University of Minnesota (Minneapolis), where he is affiliated with the Power and Energy Systems research group. His research interests include modeling, analysis, and control of power electronics and power systems with a focus on renewable integration. Dr. Dhople received the NSF CAREER Award in 2015. He currently serves as an Associate Editor for the IEEE Transactions on Energy Conversion.

Georgios B. Giannakis (Fellow'97) received his Diploma in Electrical Engr. from the Ntl. Tech. Univ. of Athens, Greece, 1981. From 1982 to 1986 he was with the Univ. of Southern California (USC), where he received his MSc. in Electrical Engineering, 1983, MSc. in Mathematics, 1986, and Ph.D. in Electrical Engr., 1986. Since 1999 he has been a professor with the Univ. of Minnesota, where he now holds an ADC Chair in Wireless Telecommunications in the ECE Department, and serves as director of the Digital Technology Center.

His general interests span the areas of communications, networking and statistical signal processing - subjects on which he has published more than 375 journal papers, 635 conference papers, 22 book chapters, two edited books and two research monographs (h-index 113). Current research focuses on learning from Big Data, wireless cognitive radios, and network science with applications to social, brain, and power networks with renewables. He is the (co-) inventor of 25 patents issued, and the (co-) recipient of 8 best paper awards from the IEEE Signal Processing (SP) and Communications Societies, including the G. Marconi Prize Paper Award in Wireless Communications. He also received Technical Achievement Awards from the SP Society (2000), from EURASIP (2005), a Young Faculty Teaching Award, the G. W. Taylor Award for Distinguished Research from the University of Minnesota, and the IEEE Fourier Technical Field Award (2015). He is a Fellow of EURASIP, and has served the IEEE in a number of posts, including that of a Distinguished Lecturer for the IEEE-SP Society.